

УДК 539.166.3

CALCULATION OF GAMMA-RAY ATTENUATION PARAMETERS FOR ALUMINIUM, IRON, ZIRCONIUM AND TUNGSTEN

H.M. Qadr

Department of Physics, College of Science, University of Raparin, Sulaimanyah, Iraqi Kurdistan, Iraq

The purpose of this study was to determine the gamma-ray linear and mass attenuation coefficients, half value layer, tenth value layer and mean free path for four shielding materials: aluminium, iron, zirconium and tungsten at the γ -rays emitted from ^{152}Eu , ^{22}Na , ^{137}Cs , and ^{60}Co radioactive sources using NaI (TI) detector. These parameters for different shielding materials were compared. The results show that tungsten is the best gamma-radiation shielding material among the materials under consideration. The measured attenuation coefficients were compared also with the theoretical values.

Key words: γ -ray attenuation coefficients, tungsten, shielding materials, half value layer, tenth value layer, mean free path.

ОПРЕДЕЛЕНИЕ ПАРАМЕТРОВ ОСЛАБЛЕНИЯ ГАММА-ИЗЛУЧЕНИЯ В АЛЮМИНИИ, ЖЕЛЕЗЕ, ЦИРКОНИИ И ВОЛЬФРАМЕ

Х.М. Кадр

Физическое отделение Научного колледжа Университета Рапарин, Сулеймания, Иракский Курдистан, Ирак

Целью данного исследования было определение линейного и массового коэффициентов ослабления γ -излучения, слоя материала, уменьшающего интенсивность γ -излучения в 2 и 10 раз, и средней длины свободного пробега фотонов в алюминии, железе, цирконии и вольфраме для γ -лучей, испускаемых радиационными источниками ^{152}Eu , ^{22}Na , ^{137}Cs и ^{60}Co с помощью NaI(Tl)- детектора. Приводится сравнение величин этих параметров, измеренных в разных поглощающих γ -излучение материалах. Результаты измерений показывают, что среди рассмотренных материалов вольфрам является наилучшим материалом, ослабляющим γ -излучение. Проведено сравнение измеренных коэффициентов ослабления γ -излучения с значениями этих коэффициентов, полученными теоретически.

Ключевые слова: коэффициенты ослабления γ -излучения, вольфрам, материалы, ослабляющие γ -излучение, средняя длина свободного пробега фотона, слой материала, уменьшающий интенсивность γ -излучения в 2 и 10 раз.

DOI: 10.21517/0202-3822-2020-43-2-25-30

INTRODUCTION

By the end of the last century, the development of nuclear technology has been climbing rapidly since the world population has increased dramatically. Approximately 16% of the world electrical power production has come from nuclear power [1—3]. Unfortunately, accidents at nuclear power plants affected the health of the population living in vicinity of these plants. Nowadays, using of γ -rays in medical diagnostics [4, 5], nuclear diagnostics, surgery, industry, agriculture and research are increasing [6, 7]. Therefore, the knowledge of γ -ray interaction with materials is gaining more importance from perspective of shielding against their effect on biological matter. Therefore, the linear and mass attenuation coefficients, half value layer (HVL), tenth value layer (TVL) and mean free path (MFP) are important parameters that must be known to designers choosing shielding materials.

Interaction of γ -rays with matter depends on the extent of γ -rays absorption or scattering, incident photon energy, type of the material and also on the geometrical conditions [8]. There are several types of the most important mechanisms of γ -ray interaction with matter. These interactions are photoelectric effect, Compton scattering and pair particles production. These interaction mechanisms cause the attenuation of the incident γ -rays [9]

During recent years, many experimental, theoretical and simulation studies have been performed on absorbed γ -dose and radiation shielding parameters in various ways, by different research groups [10—17]. The objective of this study was to determine the values of above parameters. Then, obtained values of the parameters were compared with the corresponding theoretical values of the same parameters at different energies.

EXPERIMENTAL DETAILS

Fig. 1 shows the schematic view of the experimental setup. Used radiation sources comprised radioactive elements with different energies of 244.67, 344.3 and 788.9 keV for ^{152}Eu , 511.0 keV for ^{22}Na , 661 keV for ^{137}Cs , 1171 and 1333 keV for ^{60}Co . Materials used as the shield were aluminium, iron, zirconium and tungsten. Sodium iodide NaI (TI) scintillation detector with a multi-channel analyzer (MCA) was applied in this study. The γ -ray spectra were analyzed by the maestro program.

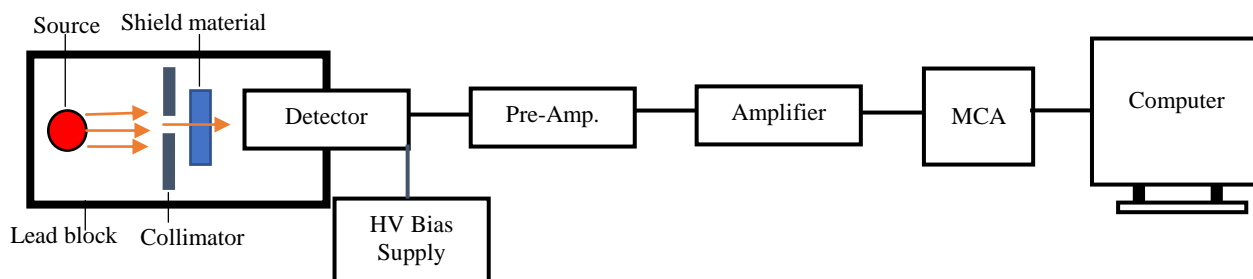


Fig. 1. Diagram of the experimental setup

Shielding materials were placed between the detector and the radioactive source. The distance between the radioactive source and the shielding material was 5 cm and the distance between the detector and the radioactive source was 9 cm. At the beginning, an initial measurement was performed without shielding material. Then the readings were recorded after passing γ -rays through the shielding materials. Data acquisition time was chosen as 5 min for each shielding material. All point measurements have been repeated five times for each shielding material.

THEORETICAL CALCULATIONS

This section summarizes background theoretical relations used for determination of linear attenuation coefficient μ , mass attenuation coefficient μ_m , HVL, TVL and MFP. According to Lambert-Beer's law, γ -rays are attenuated passing through an absorber [18]. The equation (1) describes the intensity of the transmitted beam (I) at any thickness of the absorber x , cm:

$$I = I_0 e^{-\mu x}. \quad (1)$$

Here I_0 is the unmitigated γ -beam intensity and μ , cm^{-1} is the linear γ -ray attenuation coefficient of the absorber with the thickness x , cm. The linear attenuation coefficient is related to many factors such as the shielding material, the incident γ -ray energy and the density of the material [19]. Rearrangement of equation (1) gives the following equation for the value of the γ -ray linear attenuation coefficient:

$$\mu = -\frac{\ln \frac{I}{I_0}}{x}. \quad (2)$$

The mass attenuation coefficient μ_m , cm^2/g is equal to the ratio of the linear attenuation coefficient of the absorber to its density ρ , g/cm^3 :

$$\mu_m = \frac{\mu}{\rho}. \quad (3)$$

This parameter is used in the calculations of many photon interaction parameters [20].

There are three terms generally used in the assessment of the effectiveness of radiation shielding: HVL, TVL and MFP. HVL, cm is the thickness of a shield or an absorber, at which the intensity of transmitted ray is one half of the initial intensity [21]. HVL is related to the linear attenuation coefficient value and is determined by the equation [22]:

$$\text{HVL} = \frac{\ln 2}{\mu} = \frac{0.693}{\mu}. \quad (4)$$

MFP, cm is the average distance between two successive collisions of γ -ray. It is described by the following equation [23]:

$$\text{MFP} = \frac{1}{\mu}. \quad (5)$$

The effectiveness of γ -rays shielding is also described by the TVL of the material. TVL, cm is the thickness of a shield or an absorber that attenuates a radiation beam to 10% of its initial radiation intensity level and is described by the following equation [24]:

$$\text{TVL} = \frac{\ln 10}{\mu} = \frac{2.303}{\mu}. \quad (6)$$

RESULTS AND ANALYSIS

In this study, the linear and mass attenuation coefficients, HVL, TVL and MFP of four shielding materials: aluminium, iron, zirconium and tungsten have been measured for γ -rays emitted by various radioactive sources.

Table 1 demonstrates the experimental values of the γ -ray linear attenuation coefficients for four shielding materials. They were obtained by measuring the intensities of γ -rays passed through the different absorbers. It is evident from this table that the linear attenuation coefficient for tungsten has the highest value, and for aluminium it is the lowest. The highest linear attenuation coefficient value of tungsten is connected with its high atomic number and high density, which promote γ -ray attenuation. Table 1 and Fig. 2 show that the linear γ -ray attenuation coefficients decrease with increasing incident energy. The experimental linear attenuation coefficient values were compared with the corresponding theoretical values [25—27]. Table 1 and Fig. 2 show good agreement between the experimental and theoretical values of the γ -ray linear attenuation coefficients.

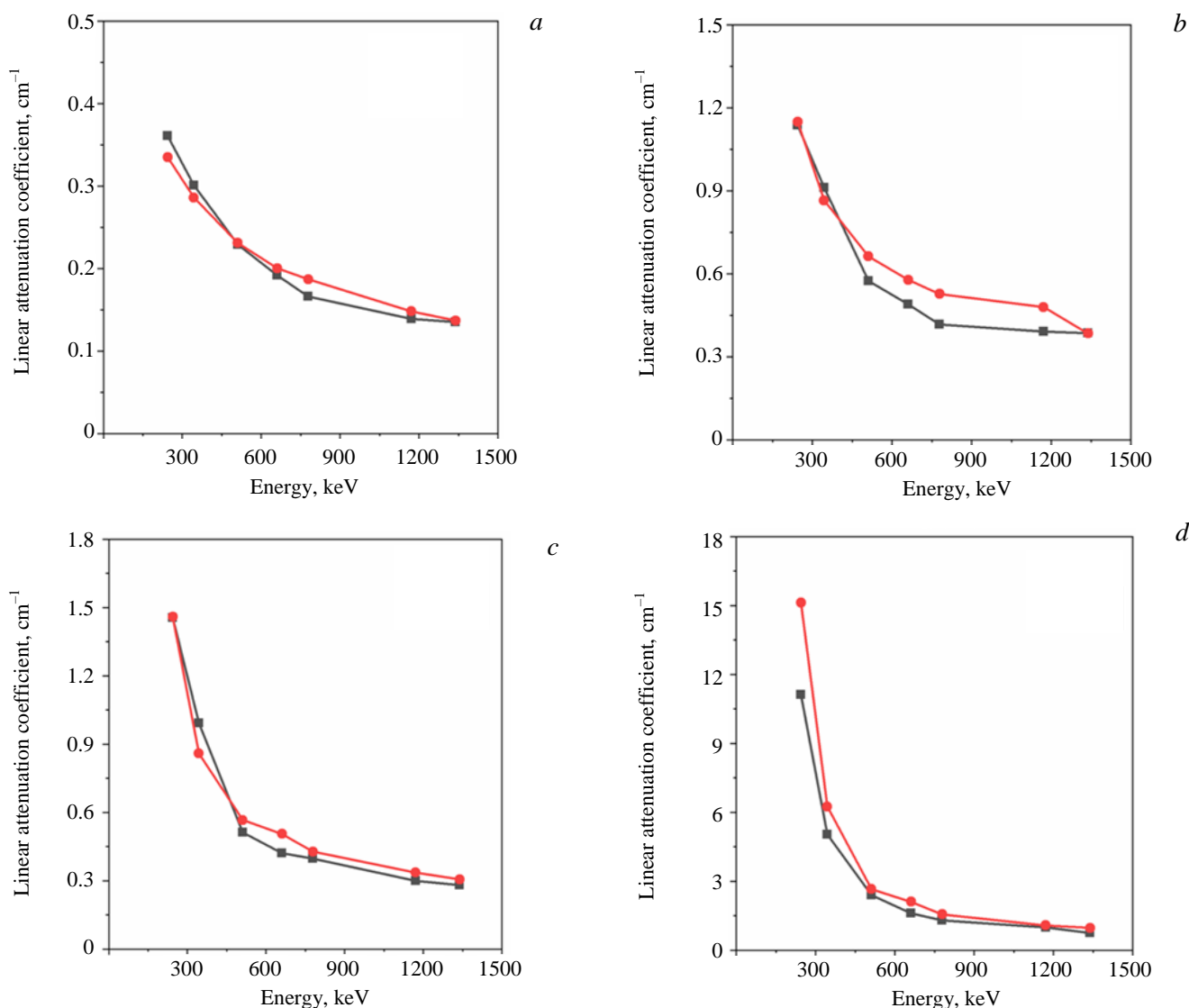


Fig. 2. The graph of linear attenuation coefficient against photon energy for four shielding materials: *a* — aluminium; *b* — iron; *c* — zirconium; *d* — tungsten; ■ — experiment; ● — theory

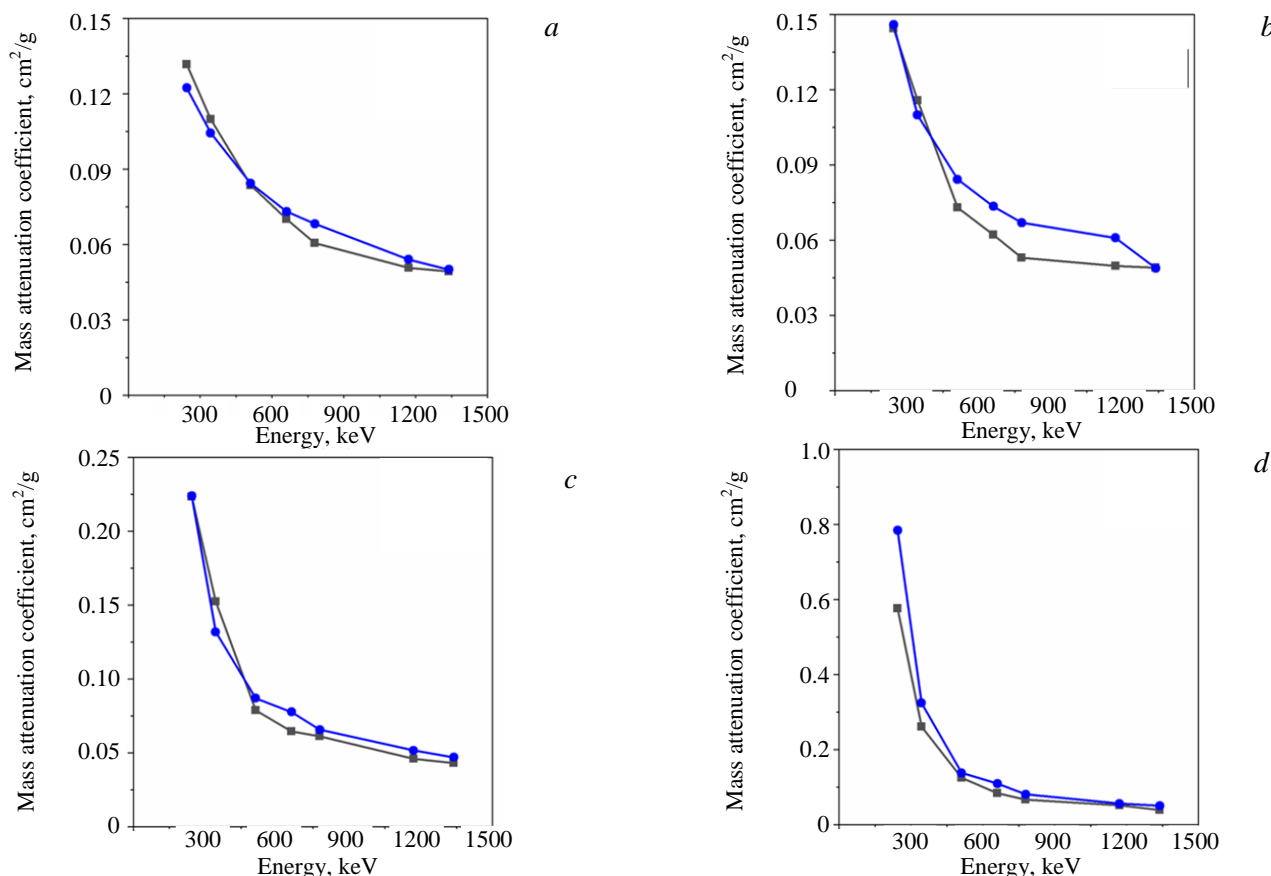
Table 1. Values of the experimental and theoretical gamma ray linear attenuation coefficients μ (cm^{-1}) for four shielding materials

Nuclides	Energy, keV	Aluminium		Iron		Zirconium		Tungsten	
		Experiment	Theory	Experiment	Theory	Experiment	Theory	Experiment	Theory
^{152}Eu	244.67	$3.61 \cdot 10^{-1}$	$3.35 \cdot 10^{-1}$	1.14	1.15	1.46	1.46	$1.11 \cdot 10^1$	$1.51 \cdot 10^1$
	344.3	$3.01 \cdot 10^{-1}$	$2.86 \cdot 10^{-1}$	$9.11 \cdot 10^{-1}$	$8.65 \cdot 10^{-1}$	$9.93 \cdot 10^{-1}$	$8.59 \cdot 10^{-1}$	5.03	6.25
^{22}Na	511.0	$2.29 \cdot 10^{-1}$	$2.31 \cdot 10^{-1}$	$5.74 \cdot 10^{-1}$	$6.63 \cdot 10^{-1}$	$5.13 \cdot 10^{-1}$	$5.67 \cdot 10^{-1}$	2.40	2.66
^{137}Cs	661.0	$1.92 \cdot 10^{-1}$	$2.00 \cdot 10^{-1}$	$4.89 \cdot 10^{-1}$	$5.78 \cdot 10^{-1}$	$4.21 \cdot 10^{-1}$	$5.06 \cdot 10^{-1}$	1.61	2.11
^{152}Eu	778.9	$1.66 \cdot 10^{-1}$	$1.87 \cdot 10^{-1}$	$4.17 \cdot 10^{-1}$	$5.27 \cdot 10^{-1}$	$3.98 \cdot 10^{-1}$	$4.28 \cdot 10^{-1}$	1.29	1.56
^{60}Co	1171	$1.39 \cdot 10^{-1}$	$1.48 \cdot 10^{-1}$	$3.91 \cdot 10^{-1}$	$4.79 \cdot 10^{-1}$	$2.99 \cdot 10^{-1}$	$3.36 \cdot 10^{-1}$	$9.93 \cdot 10^{-1}$	1.08
	1333	$1.35 \cdot 10^{-1}$	$1.37 \cdot 10^{-1}$	$3.86 \cdot 10^{-1}$	$3.84 \cdot 10^{-1}$	$2.81 \cdot 10^{-1}$	$3.06 \cdot 10^{-1}$	$7.42 \cdot 10^{-1}$	$9.65 \cdot 10^{-1}$

Another parameter measured in this study for the γ -ray interaction with materials is mass attenuation coefficient. Its values for the same four shielding materials were determined using equation (3). The experimental γ -ray mass attenuation coefficients of the shielding materials with the mentioned radioactive sources are shown in Table 2, demonstrating that tungsten also has the highest values of the γ -ray mass attenuation coefficients over all the γ -sources compared with other shielding materials due to its high atomic number and high density. The experimental and theoretical values of the mass attenuation coefficients are in good agreement [25–27]. The variation of the mass attenuation coefficients with incident γ -ray energy for the four shielding materials are represented in Fig. 3, where it is clearly shown that γ -ray mass attenuation coefficients also depend on the γ -radiation incident energy decreasing with increasing γ -ray incident energy.

Table 2. Values of the experimental and theoretical gamma ray mass attenuation coefficients μ_m (cm^2/g) for four shielding materials

Nuclides	Energy, keV	Aluminium		Iron		Zirconium		Tungsten	
		Experiment	Theory	Experiment	Theory	Experiment	Theory	Experiment	Theory
^{152}Eu	244.67	$1.32 \cdot 10^{-1}$	$1.22 \cdot 10^{-1}$	$1.44 \cdot 10^{-1}$	$1.46 \cdot 10^{-1}$	$2.23 \cdot 10^{-1}$	$2.24 \cdot 10^{-1}$	$5.76 \cdot 10^{-1}$	$7.84 \cdot 10^{-1}$
	344.3	$1.10 \cdot 10^{-1}$	$1.04 \cdot 10^{-1}$	$1.16 \cdot 10^{-1}$	$1.10 \cdot 10^{-1}$	$1.52 \cdot 10^{-1}$	$1.32 \cdot 10^{-1}$	$2.61 \cdot 10^{-1}$	$3.24 \cdot 10^{-1}$
^{22}Na	511.0	$8.36 \cdot 10^{-2}$	$8.43 \cdot 10^{-2}$	$7.29 \cdot 10^{-2}$	$8.42 \cdot 10^{-2}$	$7.87 \cdot 10^{-2}$	$8.70 \cdot 10^{-2}$	$1.24 \cdot 10^{-1}$	$1.38 \cdot 10^{-1}$
^{137}Cs	661.0	$7.01 \cdot 10^{-2}$	$7.31 \cdot 10^{-2}$	$6.21 \cdot 10^{-2}$	$7.34 \cdot 10^{-2}$	$6.46 \cdot 10^{-2}$	$7.76 \cdot 10^{-2}$	$8.35 \cdot 10^{-2}$	$1.09 \cdot 10^{-1}$
^{152}Eu	778.9	$6.06 \cdot 10^{-2}$	$6.82 \cdot 10^{-2}$	$5.30 \cdot 10^{-2}$	$6.69 \cdot 10^{-2}$	$6.10 \cdot 10^{-2}$	$6.56 \cdot 10^{-2}$	$6.69 \cdot 10^{-2}$	$8.07 \cdot 10^{-2}$
^{60}Co	1171	$5.07 \cdot 10^{-2}$	$5.40 \cdot 10^{-2}$	$4.97 \cdot 10^{-2}$	$6.08 \cdot 10^{-2}$	$4.59 \cdot 10^{-2}$	$5.15 \cdot 10^{-2}$	$5.15 \cdot 10^{-2}$	$5.58 \cdot 10^{-2}$
	1333	$4.93 \cdot 10^{-2}$	$5.00 \cdot 10^{-2}$	$4.90 \cdot 10^{-2}$	$4.88 \cdot 10^{-2}$	$4.31 \cdot 10^{-2}$	$4.69 \cdot 10^{-2}$	$3.84 \cdot 10^{-2}$	$5.00 \cdot 10^{-2}$

Fig. 3. The graph of mass attenuation coefficient against photon energy for four shielding materials: *a* — aluminium; *b* — iron; *c* — zirconium; *d* — tungsten; ■ — experiment; ● — theory

The γ -ray HVL, TVL and MFP are also important parameters in designing any radiation shielding. Their value for shielding materials under consideration are given in Fig. 4. Aluminium has the highest values of HVL, TVL and MFP, while tungsten has the lowest values of these parameters. The lower HVL, TVL and MFP values of any shielding material are better for shielding purposes. All the above-mentioned parameters are similar for the iron and zirconium, although each of these materials has different density. Fig. 4 also shows that HVL, TVL and MFP increase with increasing the incident energy, as is expected basing on the mass attenuation coefficient behavior.

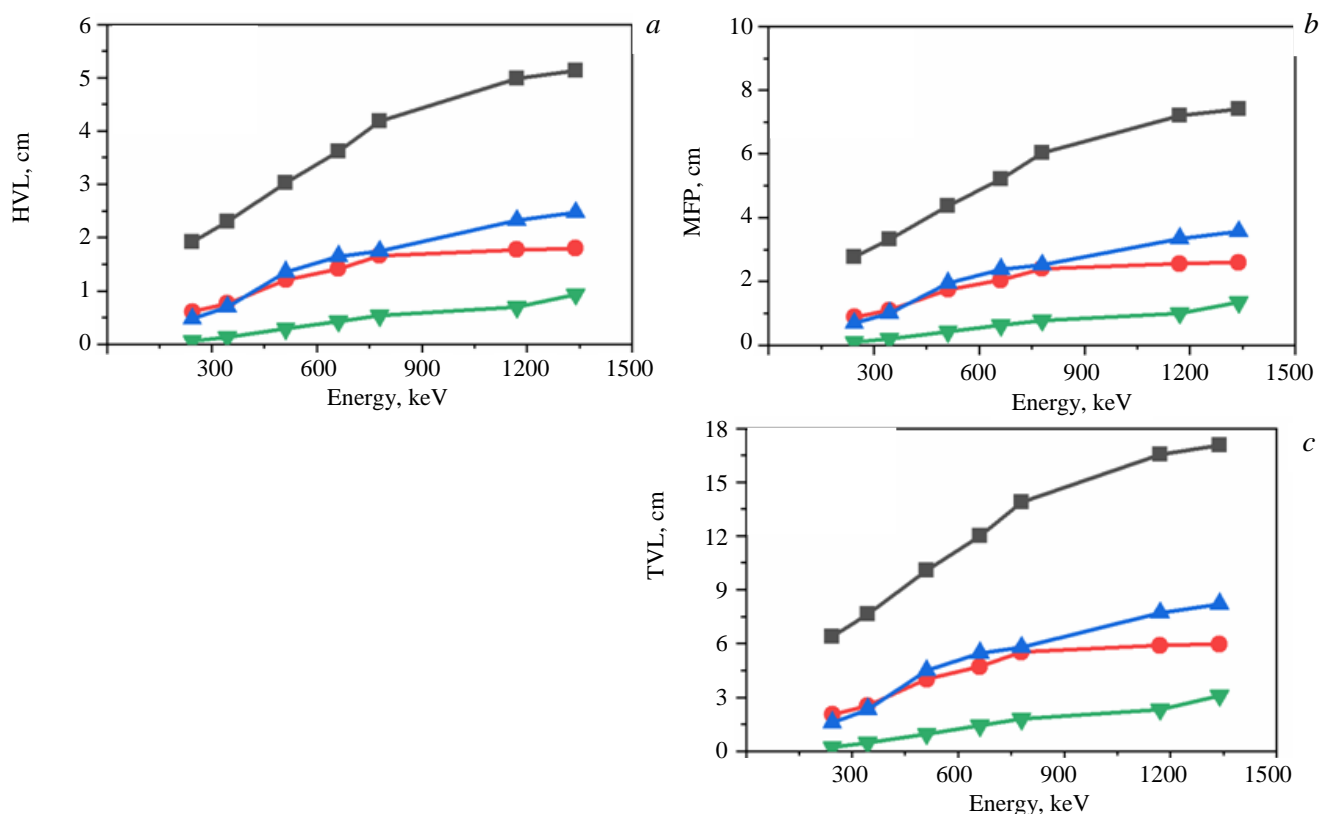


Fig. 4. Variation of HVL (a), MFP (b) and TVL (c) for four shielding materials: —■— aluminium; —●— iron; —▲— zirconium; —▼— tungsten

CONCLUSION

In the present investigation, the γ -ray attenuation properties of four shielding materials have been evaluated and discussed. The values of the linear and mass attenuation coefficients decrease with increasing incident energy. Tungsten appears to be the best γ -ray shielding material among the four materials under consideration due to its higher atomic number and density. It has the highest linear and mass attenuation coefficients compared to other considered shielding materials. The experimental results agree with the theoretical values.

The values of HVL, TVL and MFP were also determined for four materials. Aluminium absorber has the highest values of the above parameters and tungsten absorber has the lowest values. The lower HVL, TVL and MFP values of any shielding material are better for shielding purposes.

REFERENCES

1. **Qadr H.** Effect of Ion Irradiation on the Mechanical Properties of High and Low Copper. — *Atom Indonesia*, 2020, vol. 46 (1), pp. 47—51.2.
2. **Hiwa M., Ari M.** Investigation of long and short term irradiation hardening of P91 and P92 ferritic/martensitic steels. — *BAHT. Сер. Термоядерный синтез*, 2019, vol. 42 (2), pp. 81—88.
3. **Qadr H.M.** Effect of ion irradiation on the hardness properties of Zirconium alloy. — *Annals of the University of Craiova, Physics*, 2019, vol. 29, pp. 68—76.
4. **Böke A.** Linear attenuation coefficients of tissues from 1 keV to 150 keV. — *Radiation Physics and Chemistry*, 2014, vol. 102, pp. 49—59.

5. **Attenuation** Coefficient Variation as a Function of Temperature in a Cortical Bone Phantom. R.M. Souza, R. Costa-Felix, A.V. Alvarenga editors. — XXVI Brazilian Congress on Biomedical Engineering; 2019. Springer.
6. **Biswas R., Sahadath H., Mollah A.S., Huq M.F.** Calculation of gamma-ray attenuation parameters for locally developed shielding material: Polyboron. — J. of Radiation Research and Applied Sciences, 2016, vol. 9 (1), pp. 26—34.
7. **Hiwa M.Q.** Stopping power of alpha particles in helium gas. — Herald of the Bauman Moscow State Technical University. Series Natural Sciences, 2020, vol. 89 (2), pp. 117—125.
8. **Singh R., Singh S., Singh G., Thind K.S.** Gamma radiation shielding properties of steel and iron slags. — New J. of Glass and Ceramics, 2017, vol. 7, pp. 1—11.
9. **Hamad A.M., Qadr H.M.** Gamma-rays spectroscopy by using a thallium activated sodium iodide NaI (Ti). — Eurasian J. of Science and Engineering, 2018, vol. 4 (1), pp. 99—111.
10. **Agar O., Tekin H.O., Sayyed M., Korkmaz M.E., Culfa O., Ertugay C.** Experimental investigation of photon attenuation behaviors for concretes including natural perlite mineral. — Results in Physics, 2019, vol. 12, pp. 237—243.
11. **Waly E.-S.A., Fusco M.A., Bourham M.A.** Gamma-ray mass attenuation coefficient and half value layer factor of some oxide glass shielding materials. — Annals of Nuclear Energy, 2016, vol. 96, pp. 26—30.
12. **Ouda A.S., Abdel-Gawwad H.A.** The effect of replacing sand by iron slag on physical, mechanical and radiological properties of cement mortar. — HBRC J., 2017, vol. 13 (3), pp. 255—261.
13. **Ouda A.S., Abdelgader H.S.** Assessing the physical, mechanical properties, and γ -ray attenuation of heavy density concrete for radiation shielding purposes. — Geosystem Engineering, 2019, vol. 22 (2), pp. 72—80.
14. **New Method** for the Determination of the Linear Attenuation Coefficient of γ -Rays in Matter. E. Adamides, A. Kavadjiklis, S. Koutroubas, P. Koutroubas, N. Moshonas editors. — AIP Conference Proceedings, 2019. AIP Publishing.
15. **Taqi A.H., Khalil H.J.** Experimental and theoretical investigation of gamma attenuation of building materials. — J. of Nuclear and Particle Physics, 2017, vol. 7 (1), pp. 6—13.
16. **Singh V., Badiger N., Kothan S., Kaewjaeng S., Korkut T., Kim H. et al.** Gamma-ray and neutron shielding efficiency of Pb-free gadolinium-based glasses. — Nuclear Science and Techniques, 2016, vol. 27 (4), p. 103.
17. **Kilicoglu O., Tekin H.O., Singh V.P.** Determination of mass attenuation coefficients of different types of concretes using Monte Carlo method. — European J. of Science and Technology, 2019, № 15, pp. 591—598.
18. **Investigation** of Attenuation Coefficients of Some Stainless Steel and Aluminum Alloys. Z. Caner, M.Ç. Tufan editors. — AIP Conference Proceedings, 2018. AIP Publishing.
19. **Celiktas C.** A method to determine the gamma-ray linear attenuation coefficient. — Annals of Nuclear Energy, 2011, vol. 38 (9), pp. 2096—2100.
20. **Akman F., Kaçal M., Sayyed M., Karataş H.** Study of gamma radiation attenuation properties of some selected ternary alloys. — J. of Alloys and Compounds, 2019, vol. 782, pp. 315—322.
21. **Akkurt I., Başıyigit C., Akkaş A., Kilingarslan Ş., Mavi B., Giinoglu K.** Determination of some heavyweight aggregate half value layer thickness used for radiation shielding. — Acta Physica Polonica-Series A General Physics, 2012, vol. 121 (1), p. 138.
22. **Haque M., Shamsuzzaman M., Uddin M.B., Salahuddin A.Z.M., Khan R.A.** Fabrication and characterization of shielding properties of heavy mineral reinforced polymer composite materials for radiation protection. — European J. of Engineering Research and Science, 2019, vol. 4 (3), pp. 15—20.
23. **Qadr H.M.** Calculation for gamma ray buildup factor for aluminium, graphite and lead. — Intern. J. of Nuclear Energy Science and Technology, 2019, vol. 13 (1), pp. 61—69.
24. **Seenappa L., Manjunatha H., Chandrika B., Chikka H.** A study of shielding properties of X-ray and gamma in barium compounds. — J. of Radiation Protection and Research, 2017, vol. 42 (1), pp. 26—32.
25. **Hubbell J.** Photon Cross Sections, Attenuation Coefficients and Energy Absorption Coefficients. National Bureau of Standards Report NSRDS-NBS29, Washington DC, 1969.
26. **Hubbell J.H., Seltzer S.M.** Tables of X-ray Mass Attenuation Coefficients and Mass Energy-Absorption Coefficients 1 keV to 20 MeV for Elements $Z = 1$ to 92 and 48 additional Substances of Dosimetric Interest. — National Inst. of Standards and Technology-PL, Gaithersburg, MD, USA, 1995.
27. **Berger M.J., Hubbell J.** XCOM: Photon Cross Sections on a Personal Computer. — National Bureau of Standards, Washington, DC, USA, 1987.

AUTHORS

Qadr H.M. Department of Physics, College of Science, University of Raparin, Sulaimanyah, Iraqi Kurdistan, Iraq;
hiwa.physics@uor.edu.krd

Received 31 March 2020

Revised 23 April 2020

Accepted 15 May 2020

Problems of Atomic Science and Technology
Ser. Thermonuclear Fusion, 2020, vol. 43, issue 2, pp. 25—30